The precordial R ' wave: a novel discriminator between cardiac sarcoidosis and arrhythmogenic right ventricular cardiomyopathy in patients presenting with ventricular tachycardia

Hoogendoorn, J.C.; Venlet, J.; Out, Y.N.J.; Man, S.; Kumar, S.; Sramko, M.; ... ; Zeppenfeld, K.

Note: To cite this publication please use the final published version (if applicable).

The precordial R′ wave: A novel discriminator between cardiac sarcoidosis and arrhythmogenic right ventricular cardiomyopathy in patients presenting with ventricular tachycardia

Jarieke C. Hoogendoorn, MD,* Jeroen Venlet, MD,* Yannick N.J. Out, MD,*
Sumche Man, MD, PhD,* Saurabh Kumar, BSc(Med)/MBBS, PhD, FHRS,[†]
Marek Sramko, MD, PhD,[‡] Dirk G. Dechering, MD,[§] Ikutaro Nakajima, MD, PhD,[∥]
Konstantinos C. Siontis, MD,[¶#] Masaya Watanabe, MD, PhD,[**]
Yoshinori Nakamura, MD,* Usha B. Tedrow, MD, FHRS,[†] Frank Bogun, MD, PhD,[¶]
Lars Eckardt, MD,[§] Petr Peichl, MD,[‡] William G. Stevenson, MD, FHRS,[∥]
Katja Zeppenfeld, MD, PhD*

From the *Department of Cardiology, Willem Einthoven Center of Arrhythmia Research and Management,
Leiden University Medical Center, Leiden, The Netherlands, [†]Department of Cardiology, Brigham and
Women's Hospital, Boston, Massachusetts, [‡]Department of Cardiology, Institute of Clinical and
Experimental Medicine, Prague, The Czech Republic, [§]Department of Cardiology II
(Electrophysiology), University Hospital Münster, Münster, Germany, [∥]Department of Cardiology,
Vanderbilt University Medical Center, Nashville, Tennessee, [¶]Department of Cardiology, University of
Michigan, Ann Arbor, Michigan, [#]Department of Cardiovascular Medicine, Mayo Clinic, Rochester,
Minnesota, and [**]Department of Cardiology, Hokkaido University Hospital, Hokkaido, Japan.

BACKGROUND Cardiac sarcoidosis (CS) with right ventricular (RV) involvement can mimic arrhythmogenic right ventricular cardiomyopathy (ARVC). Histopathological differences may result in disease-specific RV activation patterns detectable on the 12-lead electrocardiogram. Dominant subepicardial scar in ARVC leads to *delayed* activation of areas with *reduced* voltages, translating into terminal activation delay and occasionally (epsilon) waves with a *small* amplitude. Conversely, patchy transmural RV scar in CS may lead to conduction *block* and therefore late activated areas with *preserved* voltages reflected as *preserved* R′ waves.

OBJECTIVE The purpose of this study was to evaluate the distinct terminal activation patterns in precordial leads V_1 through V_3 as a discriminator between CS and ARVC.

METHODS Thirteen patients with CS affecting the RV and 23 patients with gene-positive ARVC referred for ventricular tachycardia ablation were retrospectively included in a multicenter approach. A non–ventricular-paced 12-lead surface electrocardiogram was analyzed for the presence and the surface area of the R′ wave (any positive deflection from baseline after an S wave) in leads V_1 through V_3.

RESULTS An R′ wave in leads V_1 through V_3 was present in all patients with CS compared to 11 (48%) patients with ARVC ($P = .002$). An algorithm including a PR interval of ≥ 220 ms, the presence of an R′ wave, and the surface area of the maximum R′ wave in leads V_1 through V_3 of ≥ 1.65 mm^2 had 85% sensitivity and 96% specificity for diagnosing CS, validated in a second cohort (18 CS and 40 ARVC) with 83% sensitivity and 88% specificity.

CONCLUSION An easily applicable algorithm including PR prolongation and the surface area of the maximum R′ wave in leads V_1 through V_3 of ≥ 1.65 mm^2 distinguishes CS from ARVC. This QRS terminal activation in precordial leads V_1 through V_3 may reflect disease-specific scar patterns.

KEYWORDS Arrhythmogenic right ventricular cardiomyopathy; Cardiac sarcoidosis; Right bundle branch block; Twelve-lead surface electrocardiogram; Ventricular tachycardia

(Heart Rhythm 2021;18:1539–1547) © 2021 Heart Rhythm Society. This is an open access article under the CC BY license (http://creativecommons.org/licenses/by/4.0/).

Introduction

Arrhythmogenic right ventricular cardiomyopathy (ARVC) and cardiac sarcoidosis (CS) are the most important underlying etiologies for scar-related ventricular tachycardias (VTs) from the right ventricle (RV).[1] The clinical phenotype of CS can mimic ARVC, although they are histopathologically different.[2] It is important to distinguish the two, as a delayed diagnosis of CS may have harmful consequences.[3] Unfortunately, the diagnostic yield of endomyocardial biopsy for CS is low[4] and ^{18}F-fluorodeoxyglucose positron emission tomography (^{18}F-FDG-PET) might be negative in patients with VT referred for ablation.[5] Besides, the Task Force Criteria (TFC), developed for the diagnosis of ARVC, have poor discriminative value as they are fulfilled in up to 63%–100% of patients with CS and RV involvement.[6,7]

A right bundle branch block (RBBB) pattern on the 12-lead surface electrocardiogram (ECG) has been described in both patients with ARVC and those with CS.[1,7–10] A RBBB pattern can be caused by conduction block within the specific conduction system on different levels.[11] However, myocardial RV scar may also influence RV activation, depending on the size, transmurality, and location of the scar. The related ECG changes may therefore mimic RBBB at first sight. It has been suggested that the presence of a RBBB-like pattern in ARVC is caused by intra-RV delay rather than proximal conduction block,[8] reflected as an atypical pattern with R′/S ratio < 1 on the ECG.[12]

We hypothesized that the distinct histological scar characteristics of ARVC and CS impact RV activation resulting in different terminal activation patterns in leads V_1 through V_3. ARVC is characterized by fibrofatty replacement from the subepicardium to the subendocardium beginning at the RV base. As a result, diffuse conduction *delay* might result in delayed activation of areas with *reduced* voltages, manifested as terminal activation delay (TAD) and occasionally an (epsilon) wave with a *small* amplitude.[8,9] Contrarily, CS is characterized by nonnecrotizing granulomas, creating patchy transmural scars.[13,14] This may result in local *block* and delayed activation of areas with *preserved* voltages, reflected as an R′ wave with a higher voltage.[15] Thus, the aim of this study was to determine whether differences in terminal activation in precordial leads V_1 through V_3 on the 12-lead surface ECG can distinguish between ARVC and CS in patients presenting with scar-related RV VT.

Methods
Study population

Patients with ARVC (fulfilling TFC[16] plus pathogenic mutation) and CS with RV involvement (fulfilling Heart Rhythm Society[4] or Japanese[17] criteria) from 7 centers (Boston, Massachusetts; Hokkaido, Japan; Leiden, The Netherlands; Ann Arbor, Michigan; Münster, Germany; Nashville, Tennessee; and Prague, The Czech Republic) who presented with a VT proven or presumably from the RV and a nonpaced ECG available were eligible for inclusion. *RV VT* was defined as a VT with left bundle branch block morphology and

dominant S wave in lead V1, confirmed by a target ablation site in the RV. The study was approved by the Dutch local ethics committee (G19.005) and adhered to the Declaration of Helsinki. All patients provided preprocedural informed consent.

Data collection

From each patient, a resting non–ventricular-paced ECG (25 mm/s and 10 mm/mV) before the first ablation procedure at the institution was obtained from the medical records. Data on imaging (including echocardiography, cardiac magnetic resonance imaging, and ^{18}F-FDG-PET), biopsies, and the presence of cardiac devices were collected. Echocardiography and ^{18}F-FDG-PET performed at the time closest to the ECG (within 6 months) were selected.

Data processing

For detailed analysis of the ECG, Leiden ECG Analysis and Decomposition Software was used.[18] An 8-channel recording in comma-separated value format is input in this MATLAB program (Version 2016a, The Mathworks Inc., Natick, Massachusetts). After the detection of QRST complexes in the spatial velocity signal and baseline correction, Leiden ECG Analysis and Decomposition Software generates a default selection of beats for subsequent averaging. This selection can manually be adjusted, after which selected beats are averaged to generate a representative and low-noise averaged beat, which can be exported in pdf format. Then, measurements per lead were performed using the measurement tool in Adobe Acrobat Pro DC with 1200% zoom. If the 8-channel recording in comma-separated value format was not available, no averaged beat could be generated. In these cases, all measurements were performed for 3 consecutive beats by using Adobe and the measurements subsequently averaged per lead.

Data analysis and definitions

The PR interval and QT interval were determined in lead II or V5. The QRS width was measured from the earliest onset until the latest offset in any lead. *RBBB* was defined as QRS duration > 120 ms, with either (1) an R′ deflection in lead V1 or V2 and an S wave of greater duration than an R wave in leads I and V6 or (2) a pure dominant (notched) R wave with an R-peak time of >50 ms in lead V1 and normal R-peak time in leads V5 and V6.[19] An *atypical RBBB pattern* was defined as R′/S ratio < 1 in lead V1.[12] A QRS of >120 ms with an R′ wave in lead V1 or V2 but without an S wave of greater duration than an R wave in leads I and V6 was also considered as an atypical RBBB pattern.

Microvoltage was defined as an amplitude of <0.5 mV in all leads for the limb leads and of <1.0 mV for the precordial leads. *QRS fragmentation* (fQRS) in a QRS of ≤120 ms was defined as notching in the R wave, a notch in the nadir of the S wave, or ≥1 R′ wave in at least 2 contiguous inferior (II and II AVF), lateral (I, AVL, V5, and V6), or RV (V1 through V3) leads. In a QRS of >120 ms, fQRS was present if there

were >2 R′ waves or >2 notches in the R wave or nadir of the S wave.[20] An *R wave* was defined as any positive deflection from baseline and a notch as a change in wave front direction.

An *epsilon wave* was defined as a reproducible low-amplitude signal distinct from the QRS complex in leads V_1 through V_3.[16] TAD was measured from the nadir of the S wave to the end of the QRS in leads V_1 through V_3 in the absence of RBBB.[16] fQRS, epsilon waves, and TAD were assessed by 2 observers.

T-wave inversion (TWI) was evaluated according to the TFC as a major (TWI in leads V_1 through V_3 in the absence of RBBB) or a minor (TWI in leads V_1 and V_2 in the absence of RBBB or TWI in leads V_1 through V_4 in the presence of RBBB) criterion, and in at least 2 contiguous inferior (II, III and AVF) and lateral (I, AVL, V_5, and V_6) leads.

Surface area of the R′ wave in leads V_1 through V_3

As surrogates for the size and voltages of late activated RV areas, the presence and the surface area (SA) of the R′ wave in leads V_1 through V_3 were measured. An *R′ wave* was defined as any positive deflection from baseline after an S wave (Figure 1). The SA of the R′ wave was measured by 2 observers.

Derivation cohort vs validation cohort

Patients were consecutively assigned to a derivation and a validation group on the basis of the order of incoming data and ECGs from the centers (Online Supplemental Figure 1). With the results of the first incoming (derivation) cohort, an ECG algorithm was developed to distinguish CS from ARVC and subsequently validated in the second (validation) cohort.

Statistical analysis

Categorical variables are expressed as number and percentage and compared using the χ^2 test or Fisher exact test. Continuous variables are expressed as mean ± SD or median (interquartile range [IQR]) and compared between groups using the Student t test or Mann-Whitney U test. Receiver

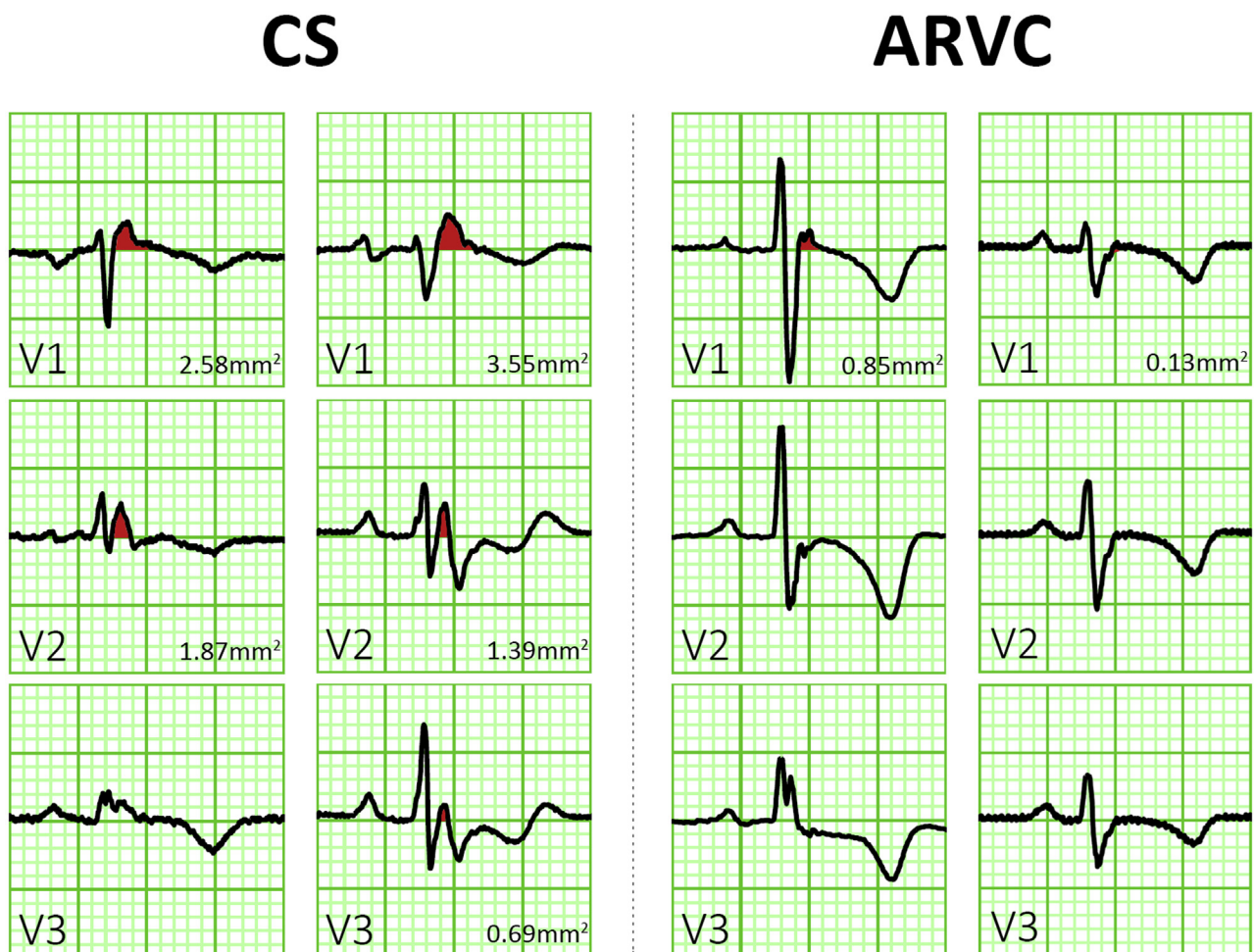**Figure 1**   Examples and surface area measurement of the R′ wave. **Left:** Two examples of the atypical R′ wave in patients with cardiac sarcoidosis (CS). Both patients with CS also fulfilled Task Force Criteria for definite diagnosis of arrhythmogenic right ventricular cardiomyopathy (ARVC). **Right:** Two patients with ARVC with small positive deflections at the end of the QRS and deep inverted T waves.

Table 1   Baseline characteristics of the derivation cohort

Characteristic	CS (n = 13)	ARVC (n = 23)
Age (y)	54 ± 8	37 ± 15
Male sex	8 (62)	18 (78)
Comorbidity		
Hypertension	2 (15)	0 (0)
Diabetes mellitus	1 (8)	0 (0)
Coronary artery disease	0 (0)	0 (0)
Antiarrhythmic drug		
Amiodarone	2 (15)	3 (13)
Sotalol	1 (8)	7 (30)
Class I	1 (8)	1 (4)
Class I and III	2 (15)	0 (0)
None	7 (54)	12 (52)
Immunosuppressive drugs	3 (23)	0 (0)
ICD	11 (85)	12 (52)
Task Force Criteria		
Structural		
Major	8 (62)	13 (57)
Minor	2 (15)	1 (4)
Tissue characterization	0/8 (0)	2/10 (20)
Arrhythmias		
Major	13 (100)	17 (74)
Minor	0 (0)	6 (26)
Family history		
Major	0 (0)	23 (100)
Minor	0 (0)	NA
Major CS criteria		
Cardiac biopsy with granulomas	3/8 (38)	0/10 (0)
LVEF < 50%	6 (46)	3 (13)
Basal thinning of interventricular septum or abnormal ventricular wall anatomy*	7 (54)	13 (57)
LGE on CMR	5/6 (83)	8/11 (73)
Focal cardiac uptake at ^{18}F-FDG-PET	5/7 (71)	0/1 (0)
High-grade atrioventricular block	1 (8)	0 (0)
Extracardiac sarcoidosis	11 (85)	0 (0)

Values are presented as mean ± SD or n (%).

ARVC = arrhythmogenic right ventricular cardiomyopathy; CMR = cardiac magnetic resonance; CS = cardiac sarcoidosis; ^{18}F-FDG-PET = ^{18}F-fluorodeoxygluose positron emission tomography; ICD = implantable cardioverter-defibrillator; LGE = late gadolinium enhancement; LVEF = left ventricular ejection fraction; NA = not applicable.

*Including ventricular aneurysm, thinning of the middle or upper ventricular septum, and regional ventricular wall thickening.

operating characteristic curve analysis was performed to determine the optimal SA cutoff of the maximum R′ wave in leads V_1 through V_3. A P value of ≤.05 was considered significant. Statistical analysis was performed using IBM SPSS version 23 (IBM Corporation, Armonk, NY).

Table 2   ECG parameters

Parameter	CS (n = 13)	ARVC (n = 23)	P
Rhythm			
Sinus rhythm	10 (77)	20 (87)	.645
Atrial pacing	3 (23)	3 (13)	
Heart rate (beats/min)	65 ± 12	61 ± 10	.246
Electrical heart axis			
Intermediate axis	10 (77)	18 (78)	.571
Left axis	3 (23)	3 (13)	
Right axis	0 (0)	2 (9)	
Conduction times			
PR interval ≥ 220 ms	4 (31)	0 (0)	.012
QRS interval > 120 ms	13 (100)	6 (26)	<.001
QTc interval (ms)	401 ± 62	425 ± 46	.194
QRS amplitudes			
Microvoltages in the limb leads	1 (8)	1 (4)	1.000
Microvoltages in the precordial leads	3 (23)	4 (17)	.686
Microvoltages in leads V_1 through V_3	8 (62)	6 (26)	.073
Epsilon wave	2 (15)	4 (17)	1.000
TAD > 55 ms*	3/3 (100)	10/22 (46)	.220
T-wave inversion			
Inferior	6 (46)	6 (26)	.281
Lateral	1 (8)	2 (9)	1.000
TFC repolarization			
Major	3 (23)	13 (57)	.143
Minor	3 (23)	2 (9)	
Surface area of the R′ wave in leads V_1 through V_3			
V_1 (mm^2)	2.85 (1.64–5.81)	0.00 (0.00–0.43)	<.001
V_2 (mm^2)	1.39 (0.16–3.26)	0.00 (0.00–0.00)	<.001
V_3 (mm^2)	0.51 (0.00–1.92)	0.00 (0.00–0.00)	.020
Maximum V_1 through V_3 (mm^2)	3.55 (2.18–5.81)	0.00 (0.00–0.43)	<.001

Values are presented as mean ± SD, median (interquartile range), or n (%).

ARVC = arrhythmogenic right ventricular cardiomyopathy; CS = cardiac sarcoidosis; QTc = corrected QT; TAD = terminal activation duration; TFC = Task Force Criteria.

*Determined in the absence of complete right bundle branch block.

Results
Study population
Thirteen patients with CS affecting the RV and 23 patients with ARVC were included in the derivation cohort (Online Supplemental Figure 1). Baseline characteristics are summarized in Table 1. The median time between ECG and mapping/ablation was 1 day (IQR 1–35 days). At the time of the ECG recording, 46% of patients with CS and 48% of patients with ARVC were on antiarrhythmic drugs.

ECG parameters

PR prolongation was present in 4 patients with CS (31%) compared with none of the patients with ARVC (Table 2). Ten patients with CS (77%) and 1 patient with ARVC (4%) fulfilled the definition of RBBB ($P < .001$); 7 of 10 patients with CS and 1 of 1 patient with ARVC had an atypical RBBB pattern with an R′/S ratio of <1. In addition, the remaining 3 patients with CS and an additional 3 patients with ARVC had a QRS duration of >120 ms and an R′ wave in lead V_1 or V_2, but did not have an S wave larger than an R wave in leads I and V_6, and therefore also had an atypical RBBB pattern.

Notably, the ECG parameters included in the TFC (epsilon wave, TAD, and repolarization abnormalities) did not differ between groups. The presence of low voltages (<1.0 mV) and/or fQRS in the RV leads (V_1 through V_3) was present in 8 patients with CS (62%) compared with 9 patients with ARVC (39%) ($P = .299$). The results of the interobserver agreement in TAD and fQRS are provided in the Online Supplemental Results and Online Supplemental Tables 1 and 2.

Presence and SA of the R′ wave in leads V_1 through V_3

Any R′ wave in leads V_1 through V_3 was present in all the 13 patients with CS compared with 11 patients with ARVC (48%) ($P = .002$). In 10 of 13 patients with CS, the R′/S ratio was <1 compared with 10 of 11 patients with ARVC. In all RV leads, the SA of the R′ wave was significantly larger in CS than in ARVC (Table 2; Online Supplementary Figure 2). The median SA of the *maximum* R′ wave in leads V_1 through V_3 was 3.55

mm^2 (IQR 2.18–5.81 mm^2) in CS and 0.00 mm^2 (IQR 0.00–0.43 mm^2) in ARVC ($P < .001$) (Figure 2A).

ECG algorithm

The SA of the maximum R′ wave in leads V_1 through V_3 was an excellent discriminator between CS and ARVC (area under the curve 0.980; 95% confidence interval 0.945–1.000; $P < .001$) (Figure 2B). An algorithm including a PR interval of ≥220 ms, the presence of an R′ wave, and the SA of the maximum R′ wave of ≥1.65 mm^2 had 85% sensitivity and 96% specificity for CS (Figure 3). The positive and negative predictive values were both 92%.

There was an excellent agreement between the 2 observers regarding the SA of the maximum R′ wave with an intraclass correlation coefficient of 0.979 (95% confidence interval 0.952–0.991; $P < .001$). The median difference between the 2 observers was 0.02 mm^2 (IQR −0.05 to 0.04 mm^2).

Validation of the ECG algorithm

The validation population included 18 patients with CS (mean age 56 ± 12 years; 67% male) and 40 patients with ARVC (mean age 38 ± 17 years; 95% male). In this group, 4 patients (3 CS and 1 ARVC) did not undergo RV mapping and the diagnosis VT of RV origin was based on the 12-lead VT morphology. The median SA of the maximum R′ wave in leads V_1 through V_3 was 4.71 mm^2 (IQR 1.14–6.68 mm^2) in CS compared with 0.23 mm^2 (IQR 0.00–0.54 mm^2) in ARVC ($P < .001$) (Figure 4A). The ECG algorithm showed 83% sensitivity and 88% specificity for CS (Figure 4B) in
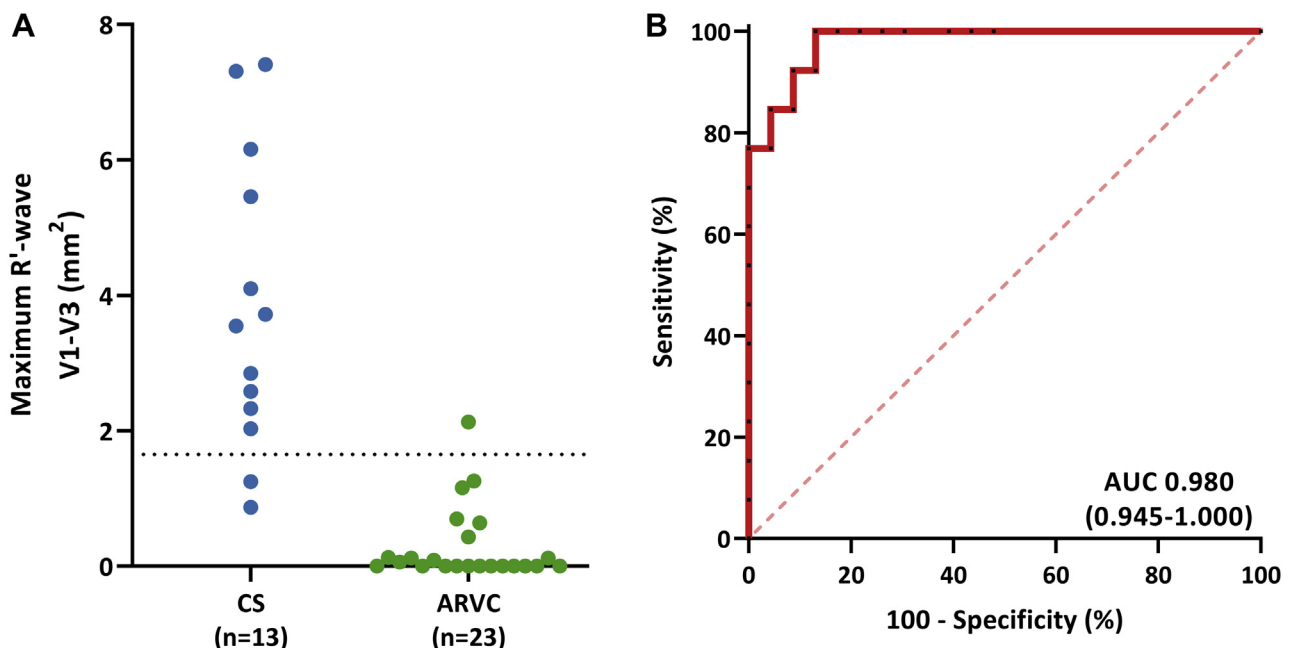

Figure 2   Surface area of the maximum R′ wave in leads V_1 through V_3. **A:** Scatterplot showing the surface area of the maximum R′ wave in leads V_1 through V_3 between cardiac sarcoidosis (CS) and arrhythmogenic right ventricular cardiomyopathy (ARVC). **B:** Results of the receiver operator characteristic curve analysis, with an excellent area under the curve (AUC). A surface area cutoff of ≥ 1.65 mm^2 had 85% sensitivity 85% and 96% specificity for diagnosing CS.
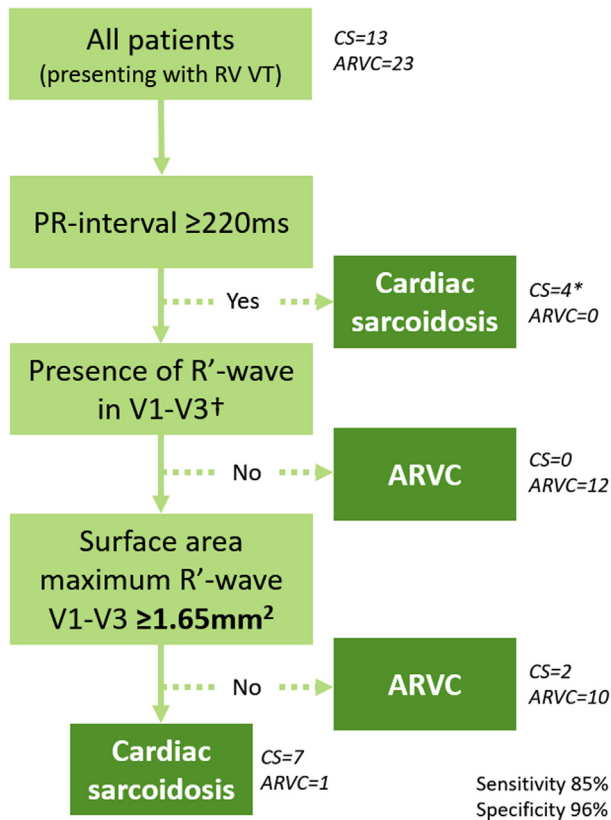
Figure 3 Twelve-lead electrocardiographic algorithm distinguishing cardiac sarcoidosis (CS) from arrhythmogenic right ventricular cardiomyopathy (ARVC) in patients with sustained ventricular tachycardia (VT) from the right ventricle (RV). *In all 4 patients with a PR interval of ≥220 ms, the surface area of the maximum R′ wave was ≥1.65 mm². †Defined as any positive deflection after an S wave.

this group (positive predictive value 75%; negative predictive value 92%).

Discussion

This study aimed to determine the role of the ECG in distinguishing CS from ARVC in patients presenting with scar-related RV VT. The main findings are as follows: (1) an easily applicable algorithm including PR prolongation, the presence of an R′ wave, and the SA of the maximum R′ wave in leads V_1 through V_3 distinguishes CS from ARVC with excellent sensitivity and specificity in both the derivation and validation cohorts and (2) the "RBBB-like" pattern in CS appears to be often atypical, suggesting that it may be at least partly due to conduction block caused by myocardial scar rather than involvement of the proximal specific conduction system.

Activation sequence of the RV

Normal RV activation starts at the apical anteroseptum and the moderator band and rapidly reaches the basal regions. It progresses from the endocardium to the epicardium, taking 60–70 ms to complete.[9,21] Myocardial scar might alter this activation sequence and duration, hence changing QRS

morphology and (localized) QRS duration on the 12-lead ECG.

The histopathologically and electroanatomically distinct myocardial scars in CS and ARVC may differently impact RV activation and the electroanatomical characteristics of late activated areas. In CS, granuloma formation leads to patchy, well-demarcated, and often transmural RV scars.[14] These confluent granulomas can cause localized conduction block. Subsequently, downstream activated areas with *preserved* voltages may be delayed activated, leading to a delayed and prolonged deflection on the ECG of considerable size.[15] In ARVC, progressive subepicardial fibrofatty replacement may also cause prolonged RV activation, in particular causing late (independent) activation of the affected low-voltage areas, typically involving the peritricuspid region.[8,9] This delayed activation may lead to the TAD and occasionally to a late deflection of low amplitude (epsilon wave). Therefore, in order to distinguish between the two etiologies, we analyzed the SA of any positive deflection (R′ wave) after an S wave in leads V_1 through V_3.

Indeed, an SA of the maximum R′ wave in leads V_1 through V_3 of ≥1.65 mm2 was a good discriminator between CS and ARVC. Although in almost half of the patients with ARVC a late positive deflection was visible, the SA of this deflection was clearly larger in CS. Figure 5 provides an example of electroanatomical activation and voltage mapping in a patient with ARVC, supporting that the small late positive deflection in lead V1 ("epsilon wave") corresponds to delayed activation of a low-voltage area.

RBBB pattern

Although a RBBB pattern is a relatively common finding in patients without structural heart disease, it has more frequently been described in patients with RV cardiomyopathy. Up to 67% of patients with CS[1,7] and up to 20% of patients with ARVC (fulfilling TFC) presenting with RV VT have a RBBB-like pattern on their ECG.[1,8–10] It is a minor criterion for the diagnosis of CS,[17] while it complicates the diagnosis of ARVC, as TWI and TAD cannot be assessed in the presence of RBBB.[16] Therefore, one prior study aimed to distinguish a RBBB pattern in ARVC from normal controls.[12] In that study, an R′/S ratio of <1 showed 88% sensitivity and 86% specificity to distinguish ARVC from normal controls. This atypical RBBB pattern in ARVC has been attributed to intra-RV delay caused by mutations in the cardiac desmosome affecting cell coupling rather than primary conduction disease.[8]

In this context, it is important to mention that all but one study investigating RBBB patterns in ARVC have included patients according to TFC and therefore also patients with right-sided CS with false-positive TFC might have been included.[7]

Intra-RV delay in ARVC has been suggested as explanation for this atypical RBBB pattern. Indeed, in ARVC peritricuspid and subepicardial involvement predominates and *delayed* transmural activation from the endocardium to the
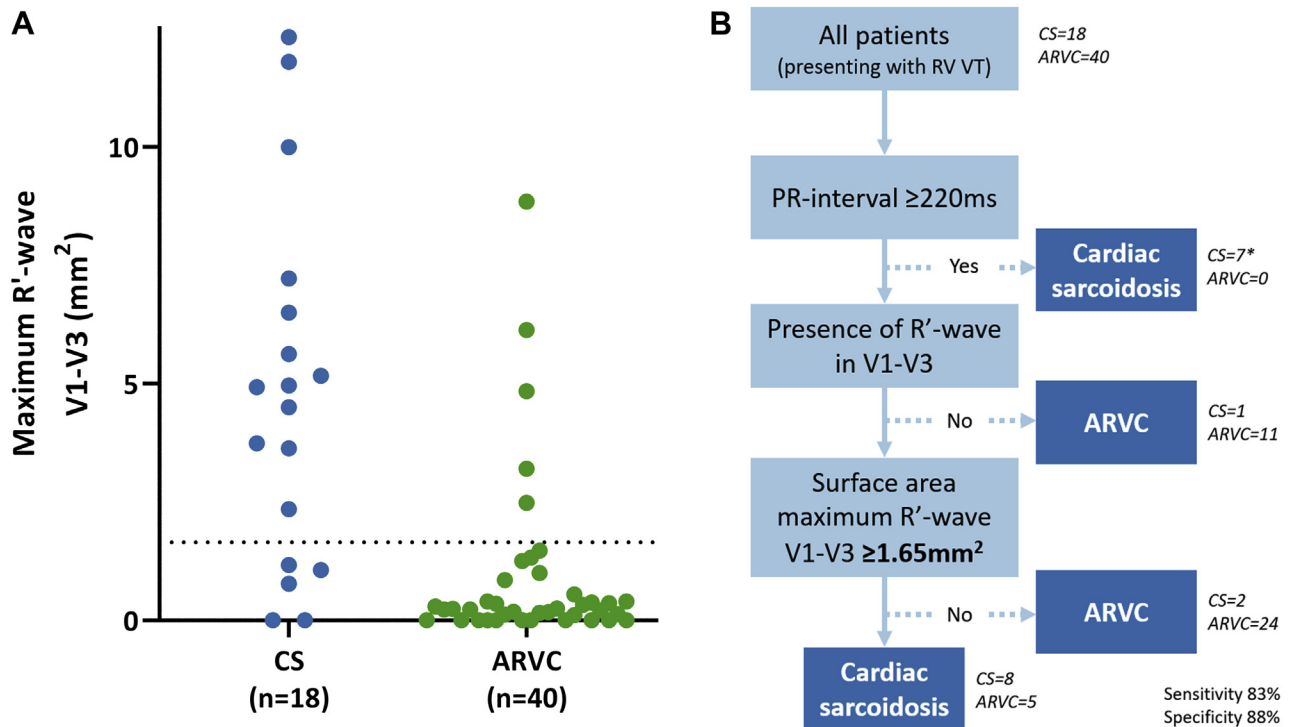
Figure 4   Surface area of the maximum R′ wave in leads V_1 through V_3 and the developed algorithm in a validation cohort. **A:** Scatterplot showing the surface area of the maximum R′ wave in leads V_1 through V_3 in a validation cohort. **B:** The developed algorithm has 83% sensitivity and 88% specificity in a large validation cohort. *In 5 of 7 patients with cardiac sarcoidosis (CS) with a PR interval of $\geq$220 ms, the surface area of the maximum R′ wave in leads V_1 through V_3 was $\geq$1.65 mm². ARVC = arrhythmogenic right ventricular cardiomyopathy; RV = right ventricle; VT = ventricular tachycardia.

epicardium has been reported.[9] Delayed transmural activation in affected areas may explain the slurring of the S wave upstroke (Figure 5) or low-amplitude late deflections, but is unlikely to cause a large-sized R′ wave, as observed in CS (Figure 6).

Prior studies have described different characteristics in patients with ARVC (fulfilling TFC 2010) with and without a RBBB pattern. Interestingly, patients with RBBB were older, had more RV dilatation, and had a lower RV ejection fraction.[12] Moreover, among patients with RBBB, 77% developed biventricular heart failure during follow-up.[22] Hence, it is interesting to speculate that some previously reported patients with ARVC and a RBBB-like pattern may have had CS, with a known more progressive course and poorer outcome.[1,7]

Level of block in patients with CS
There are 3 types of RBBB, namely, proximal, distal, and terminal.[11] Although in CS a proximal RBBB might be present because of granulomas involving the proximal right fascicle, it is also possible that in CS a RBBB pattern is caused by confluent dense and transmural myocardial RV free wall scar leading to late activation of the preserved peritricuspid region. In more than half of the patients with CS and a RBBB-like pattern on their ECG, this pattern was atypical with an R′/S ratio of <1 or an S wave shorter than an R wave in leads I and V6, suggesting that

this might not be typical proximal RBBB. In addition, it is known from postsurgical studies that even block on a distal or terminal level can mimic typical ECG RBBB.[11] Thus, it is interesting to speculate that transmural myocardial scar in CS may mimic typical RBBB, even when the scar location is more distal. However, subtle differences need to be appreciated.

Figure 6 provides an example of a patient with CS who fulfilled TFC for definite ARVC, who had a preserved R′ wave in leads V_1 through V_3, and who underwent electroanatomic mapping. There is conduction block in the septal RV outflow tract. Figure 6B shows a right fascicle potential and therefore proximal RBBB is unlikely. The R′ wave and second late deflection are caused by delayed activation of areas with relatively preserved voltages.

Clinical implications and future perspectives
Recognition of the ECG pattern described in this study should raise the suspicion for CS in patients presenting with scar-related RV VT and should prompt further investigations (such as ^{18}F-FDG-PET and/or biopsies) even in the absence of other features related to CS. In addition, the ECG pattern described in this study may indicate RV involvement with a higher propensity for ventricular arrhythmias, warranting careful diagnostic testing and follow-up.[23] Last, in most of the patients, extracardiac
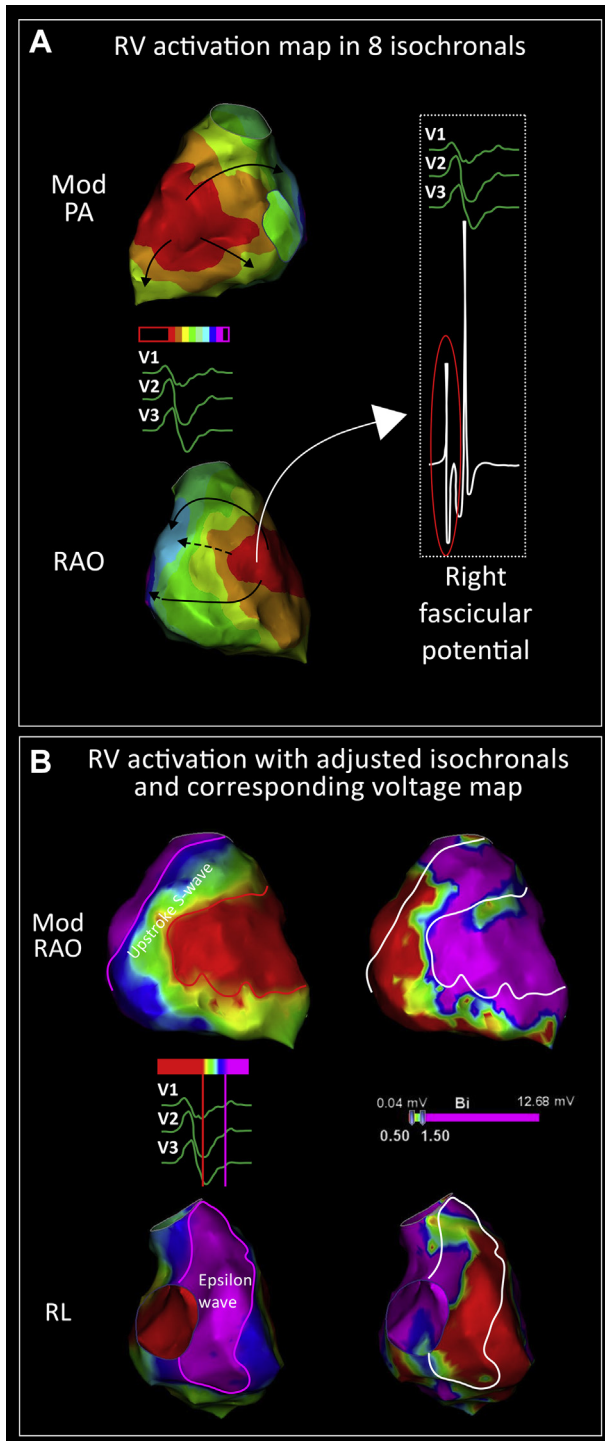
Figure 5 Right ventricular (RV) endocardial electroanatomic map of a 52-year-old man with arrhythmogenic right ventricular cardiomyopathy. **A:** Activation map of the RV in 8 isochronals color coded according to the bar. There is no conduction block but evidence for conduction slowing at the basal free wall toward the peritricuspid area (*dashed arrow*). The insert panel shows a potential from the distal right fascicle (moderator band) excluding proximal right bundle branch block. **B:** RV activation with adjusted isochronals according to the electrocardiogram (*yellow to blue* reflects the upstroke of the S wave in lead V₁, and *purple* indicates the epsilon wave) with the corresponding bipolar voltage map. The upstroke of the S wave coincides with slow activation of the free wall. The epsilon wave coincides with late activation of the basoinferior segment with reduced voltages. The propagation map of this patient is available in Online Supplemental Movie 1. Mod PA = modified posteroanterior; Mod RAO = modified right anterior oblique; RAO = right anterior oblique; RL = right lateral.
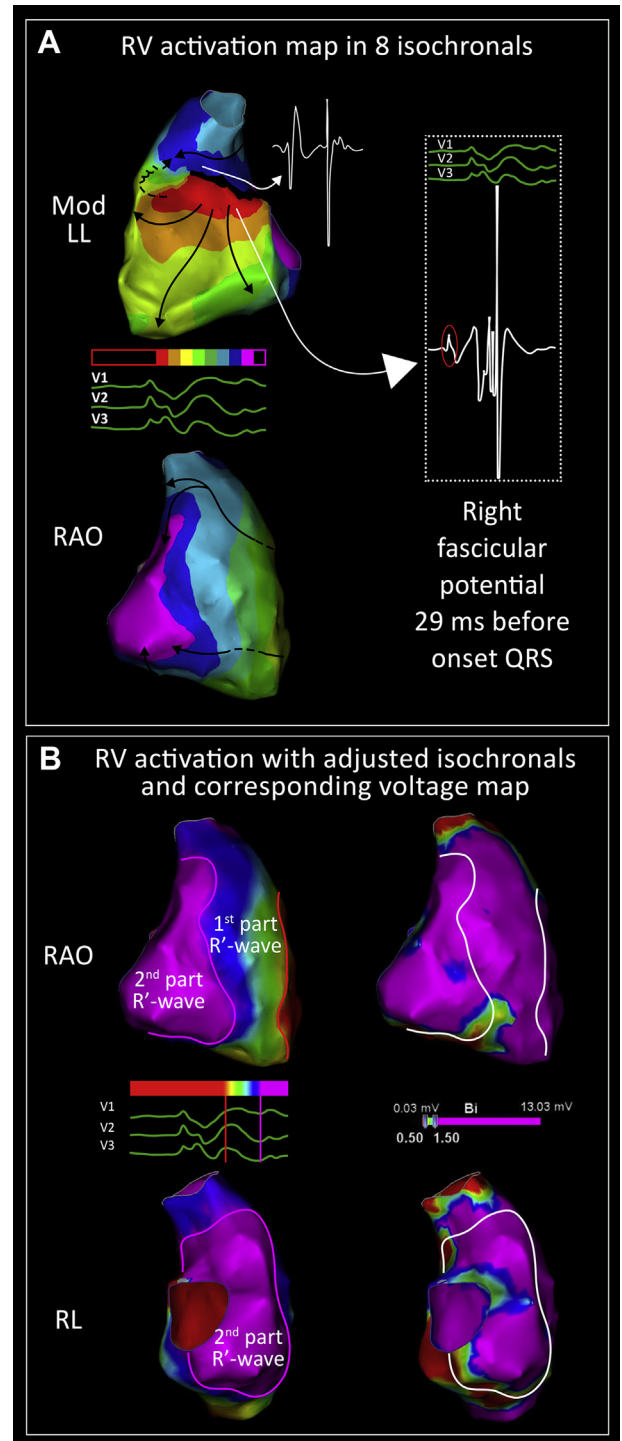
Figure 6 Right ventricular (RV) endocardial electroanatomic map of a 49-year-old woman with cardiac sarcoidosis. **A:** Activation map of the RV in 8 isochronals color coded according to the bar. There is a line of conduction block in the septal RV outflow tract (*black line*). As a result, the infundibulum is activated from the anterior segment. The insert panel shows a potential from the distal right fascicle and therefore proximal right bundle branch block is unlikely. **B:** RV activation with adjusted isochronals according to the electrocardiogram (*yellow to blue* reflects the first part of the R′ wave in lead V₁, and *purple* indicates the second part of the R′ wave) with the corresponding bipolar voltage map. The second R′ wave coincides with late activation of the basoinferior segment, with relatively preserved voltages. The propagation map of this patient is available in Online Supplemental Movie 2. Mod LL = modified left lateral; RAO = right anterior oblique; RL = right lateral.

sarcoidosis is asymptomatic and only diagnosed after sus-picion of CS.[3] Therefore, (extra)cardiac sarcoidosis needs to be suspected before adequate tests will be initiated. The ECG algorithm may be of help in initializing additional diagnostic tests.

Future longitudinal studies are needed to determine the time course of the development of these specific ECG fea-tures. It would be interesting to evaluate if they might predict initial VT occurrence. In this regard, it is important to mention that 1 study reported worse outcome for patients who *developed* a RBBB-like pattern compared with those who already had this QRS pattern at baseline.[22]

Limitations
First, this is a retrospective cross-sectional study. However, it is multicenter and a validation cohort was included. Second, the study included patients referred for VT ablation to tertiary centers, which might reflect a more advanced stage of disease and/or a specific scar pattern related to VT. Third, the cutoff provided in this study ($1.65 mm^2$ on an ECG with 25 mm/s) might be difficult to assess visually. However, a cutoff of $2.00 mm^2$ has the same sensitivity and specificity and might be easier to apply in clinical practice (Figures 2 and 4). To use this parameter irrespective of the sweep speed, a cutoff of 6.6 or 8.0 ms·mV can be used, respectively.

Conclusion
The SA of the maximum R′ wave in leads V_1 through V_3 of $\geq 1.65 mm^2$ discriminates between CS with RV involvement and ARVC in patients presenting with scar-related RV VT. This likely reflects different scar patterns, with transmural RV scars in CS leading to conduction block and subepicar-dial scars in ARVC leading to conduction delay. The pres-ence of this ECG pattern should prompt careful consideration of diagnostic testing for CS.

Appendix
Supplementary data
Supplementary data associated with this article can be found in the online version at https://doi.org/10.1016/j.hrthm.2021. 04.032.

References

1. Kumar S, Baldinger SH, Kapur S, et al. Right ventricular scar-related ventricular tachycardia in nonischemic cardiomyopathy: electrophysiological characteristics, mapping, and ablation of underlying heart disease. J Cardiovasc Electrophysiol 2018;29:79–89.
2. Vasaiwala SC, Finn C, Delpriore J, et al. Prospective study of cardiac sarcoid mimicking arrhythmogenic right ventricular dysplasia. J Cardiovasc Electrophysiol 2009;20:473–476.
3. Hoogendoorn JC, Ninaber MK, Piers SRD, et al. The harm of delayed diagnosis of arrhythmogenic cardiac sarcoidosis: a case series. Europace 2020; 22:1376–1383.
4. Birnie DH, Sauer WH, Bogun F, et al. HRS expert consensus statement on the diagnosis and management of arrhythmias associated with cardiac sarcoidosis. Heart Rhythm 2014;11:1305–1323.
5. Muser D, Santangeli P, Liang JJ, et al. Characterization of the electroanatomic substrate in cardiac sarcoidosis: correlation with imaging findings of scar and inflammation. JACC Clin Electrophysiol 2018;4:291–303.
6. Dechering DG, Kochhäuser S, Wasmer K, et al. Electrophysiological charac-teristics of ventricular tachyarrhythmias in cardiac sarcoidosis versus ar-rhythmogenic right ventricular cardiomyopathy. Heart Rhythm 2013; 10:158–164.
7. Philips B, Madhavan S, James CA, et al. Arrhythmogenic right ventricular dysplasia/cardiomyopathy and cardiac sarcoidosis: distinguishing features when the diagnosis is unclear. Circ Arrhythm Electrophysiol 2014; 7:230–236.
8. Tanawuttiwat T, Te Riele AS, Philips B, et al. Electroanatomic correlates of de-polarization abnormalities in arrhythmogenic right ventricular dysplasia/cardio-myopathy. J Cardiovasc Electrophysiol 2016;27:443–452.
9. Haqqani HM, Tschabrunn CM, Betensky BP, et al. Layered activation of epicardial scar in arrhythmogenic right ventricular dysplasia: possible sub-strate for confined epicardial circuits. Circ Arrhythm Electrophysiol 2012; 5:796–803.
10. Kubala M, Pathak RK, Xie S, et al. Electrocardiographic repolarization abnormal-ities and electroanatomic substrate in arrhythmogenic right ventricular cardiomy-opathy. Circ Arrhythm Electrophysiol 2018;11:e005553.
11. Horowitz LN, Alexander JA, Edmunds LH Jr. Postoperative right bundle branch block: identification of three levels of block. Circulation 1980;62:319–328.
12. Jain R, Dalal D, Daly A, et al. Electrocardiographic features of arrhythmogenic right ventricular dysplasia. Circulation 2009;120:477–487.
13. Kumar S, Barbhaiya C, Nagashima K, et al. Ventricular tachycardia in cardiac sarcoidosis: characterization of ventricular substrate and outcomes of catheter ablation. Circ Arrhythm Electrophysiol 2015;8:87–93.
14. Tavora F, Cresswell N, Li L, et al. Comparison of necropsy findings in patients with sarcoidosis dying suddenly from cardiac sarcoidosis versus dying suddenly from other causes. Am J Cardiol 2009;104:571–577.
15. Santucci PA, Morton JB, Picken MM, Wilber DJ. Electroanatomic mapping of the right ventricle in a patient with a giant epsilon wave, ventricular tachy-cardia, and cardiac sarcoidosis. J Cardiovasc Electrophysiol 2004; 15:1091–1094.
16. Marcus FI, McKenna WJ, Sherrill D, et al. Diagnosis of arrhythmogenic right ventricular cardiomyopathy/dysplasia: proposed modification of the Task Force Criteria. Circulation 2010;121:1533–1541.
17. Terasaki F, Yoshinaga K. New guidelines for diagnosis of cardiac sarcoidosis in Japan. Ann Nucl Cardiol 2017;3:42–45.
18. Draisma HHM, Swenne CA, Van De Vooren H, et al. LEADS: an interactive research oriented ECG/VCG analysis system. Comput Cardiol 2005; 32:515–518.
19. Surawicz B, Childers R, Deal BJ, et al. AHA/ACCF/HRS recommendations for the standardization and interpretation of the electrocardiogram: part III: intraven-tricular conduction disturbances: a scientific statement from the American Heart Association Electrocardiography and Arrhythmias Committee, Council on Clin-ical Cardiology; the American College of Cardiology Foundation; and the Heart Rhythm Society. Endorsed by the International Society for Computerized Electro-cardiology. J Am Coll Cardiol 2009;53:976–981.
20. Das MK, Zipes DP. Fragmented QRS: a predictor of mortality and sudden cardiac death. Heart Rhythm 2009;6:S8–S14.
21. Durrer D, van Dam RT, Freud GE, et al. Total excitation of the isolated human heart. Circulation 1970;41:899–912.
22. Peters S, Trümmel M, Koehler B. Special features of right bundle branch block in patients with arrhythmogenic right ventricular cardiomyopathy/dysplasia. Int J Cardiol 2012;157:102–103.
23. Velangi PS, Chen KA, Kazmirczak F, et al. Right ventricular abnormalities on cardiovascular magnetic resonance imaging in patients with sarcoidosis. JACC Cardiovasc Imaging 2020;13:1395–1405.